# Evacuated glazing with tempered glass

**Fang, Y. & Arya, F.**



**Original citation & hyperlink:**
Fang, Y & Arya, F 2019, 'Evacuated glazing with tempered glass' Solar Energy, vol. 183, pp. 240-247.
https://dx.doi.org/10.1016/j.solener.2019.03.021

DOI 10.1016/j.solener.2019.03.021
ISSN 0038-092X
ESSN 1471-1257

Publisher: Elsevier

# Evacuated Glazing with Tempered Glass

Yueping Fang[*1], Farid Arya[2]

[1]Centre for Research in the Built and Natural Environment,

School of Energy, Construction and Environment, Coventry University

Priory Street, CV1 5FB, Coventry, UK

[2]Centre for Sustainable Technologies, Ulster University,

Shore Road, Newtownabbey, BT37 0QB, Northern Ireland, UK

**Abstract:** The application of tempered glass has made it possible to significantly reduce the support pillar number within evacuated glazing (EG) since tempered glass (T-glass) is four to ten times mechanically stronger than annealed glass (A-glass). The thermal transmittance (U-value) of 0.4 m by 0.4 m double evacuated glazing (DEG) with 4 mm thick T-glass and A-glass panes with emittance of 0.03 were determined to be 0.3 $Wm^{-2}K^{-1}$ and 0.57 $Wm^{-2}K^{-1}$, respectively (47.4% improvement) using previously experimentally validated finite volume model. The thermal transmittance (U-value) of 0.4 m by 0.4 m triple evacuated glazing (TEG) with 4 mm thick T-glass and A-glass panes with emittance of 0.03 were determined to be 0.11 $Wm^{-2}K^{-1}$ and 0.28 $Wm^{-2}K^{-1}$, respectively (60.7% improvement). The improvement in the U-value of EG with T-glass is due to a reduction in support pillar number, leading to reduction in heat conduction through pillar array. The impact of tempered glass on the thermal transmittance for TEG is greater than that of DEG since radiative heat transfer in TEG is much lower than that in DEG, thus the reduction in heat conduction resulted from the reduction of support pillar number in TEG is much larger than that in DEG.

**Key words**: Evacuated glazing, Annealed glass (A-glass); Tempered glass (T-glass), thermal performance, support pillars

## 1. Introduction

Buildings were responsible for approximately 40% of the total energy consumption in 2014 in the EU according to a recent International Energy Agency (IEA) report (Cuce and Cuce, 2016). Windows are generally considered the weakest component of the building in terms of energy efficiency, and can contribute to 60% of energy loss in the buildings (Jelle et al., 2012; Manz and Menti, 2012). Significant

[*] Corresponding author. Tel: +44 24 77650889. Email address: yueping.fang@coventry.ac.uk; fangyueping@hotmail.com (Y. Fang)

research (Cuce et al., 2015, 2016) has been undertaken to reduce the thermal transmission U-value of windows, such as multi-layer glazing (Wang and Wang, 2016), suspended particle device switchable glazing (Ghosh et al., 2016), glazing with suspended films (Frost et al., 1996, ), vacuum glazing (Manz, 2008; Collins and Simko, 1998; Fang et al., 2014; Arya, 2014), triple vacuum glazing (Fang et al., 2015), aerogel glazing (Schultz et al., 2005) and hybrid vacuum glazing (Fang et al., 2013). A range of smart glazing technologies have been developed to provide thermal and visual comfort and generate electricity, such as electrochromic vacuum glazing (Fang et al., 2014), insulating glazing with integrated blinds embedded with cooling pipes (Shen, 2016), heat insulating solar glass (Cucu et al., 2016), and PV glazing (Fung and Yang, 2008; Peng et al., 2016; Wang et al., 2017). Amongst these glazing technologies evacuated glazing (EG) provides a promising solution for reducing heat loss through windows due to its extremely low U-value (1 $Wm^{-2}K^{-1}$), high solar heat gain (0.66) and thinner profile (8.15 mm) compared to other systems (Zhao et al., 2007; Pilkington, 2019).

Significant theoretical and experimental work have been done for EG sealed by solder glass and indium alloy as sealant (Collins and Simko, 1998; Fang et al., 2016). The solder glass technique is well-established and has been used by Nippon Sheet Glass and AGC for commercialized EG. The melting point of typical solder glass is about 450ºC which restricts the application of tempered glass (T-glass) into evacuated glazing since at such high temperature T-glass will lose its temper qualities. However, applying T-glass into evacuated glazing can significantly reduce the number of support pillars since T-glass is four to ten times stronger than annealed glass. The lower the pillars number, the lower the heat flow through the pillars within evacuate glazing. However, support pillar specifications should satisfy the safety requirements outlined by Collins et al. (1992) which are summarized in Figure 1 where external tensile stress on the glass surface right above pillars is less than 4 MPa, the overall thermal conductance of support pillar array is below 0.3 $Wm^{-2}K^{-1}$ and conical fractures near support pillar do not occur. Pillar separation and radius chosen from the shaded region presented in Figure 1 can satisfy the safety requirements (Collins et al., 1992).

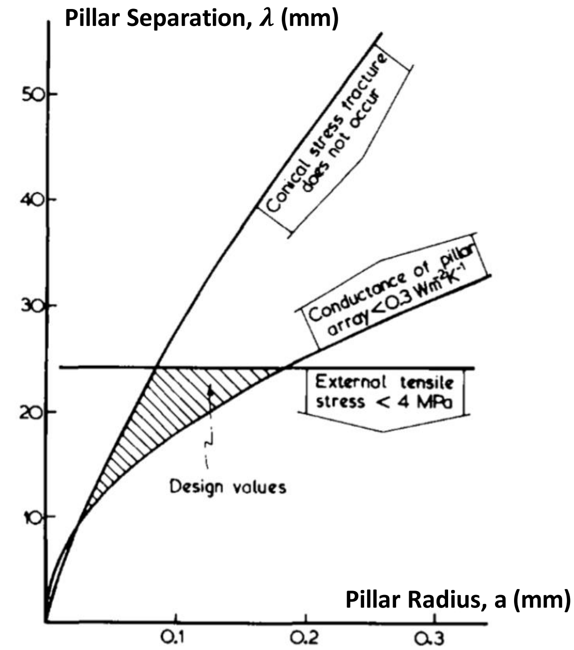


Fig. 1 Support pillar design constraints (Collins et al., 1992).

Due to higher mechanical strength of T-glass compared to that of A-glass, T-glass can meet the safety requirements, consequently, extensive work has been undertaken to reduce the melting point of solder glass achieving a minimum melting point of 380ºC to date. Panasonic Company has commercialized evacuated glazing with T-glass using this technique. This temperature is still too high for tempered glass panes as their temper quality will degrade at this temperature. To avoid this issue the sealing temperature should be below 200℃ (Hyde et al., 2000). Using ultrasonic soldering techniques, Hyde et al. (2000) successfully fabricated DEG samples using indium as a sealing material with a melting temperature of about 156°C. Using this fabrication process it is possible to use tempered glass panes in the fabrication of EG enabling the increase of the distance between support pillars and the decrease of pillars number resulting in fewer contact points between the two glass panes.

LandVac Glass company has independently developed a low temperature sealing technique and used in their production line for evacuated glazing and now the company has a big portion of glazing market in China (LandVac, 2019). Both techniques have been proved to be viable for T-glass evacuated glazing, but both have advantages and disadvantages which will be discussed in our future paper. Apart from the work undertaken at Ulster University on TEG (Fang et al., 2015), there is little report in the literature on the fabrication of TEG. In this paper, therefore, the potential thermal performance of DEG and TEG with

T-glass under ISO (2017) winter conditions is investigated. This work will contribute to the development and application of evacuated glazing with T-glass since many building codes require the use of T-glass.

## 2. Methodology

### 2.1 Heat transfer through DEG and TEG

Figures 2 shows the configurations (not to scale) of DEG which comprise two A-glass (Fig. 2a) and two T-glass (Fig. 2b). The pillar separation of the DEG in Fig. 2(b) with T-glass glass is twice those of the DEG with A-glass in Fig. 2(a). Figures 3 shows the configurations (not to scale) of TEG which comprise three A-glass (Fig. 2a) and three T-glass (Fig. 2b). The pillar separation of the TEG in Fig. 3(b) with T-glass glass is twice those of the TEG with A-glass in Fig. 3(a). Heat conduction though pillar arrays and edge seal, radiative heat transfer between internal surfaces of vacuum gap, convective heat transfer on the warm and code side glass surfaces are presented in Figs. 2 and 3.

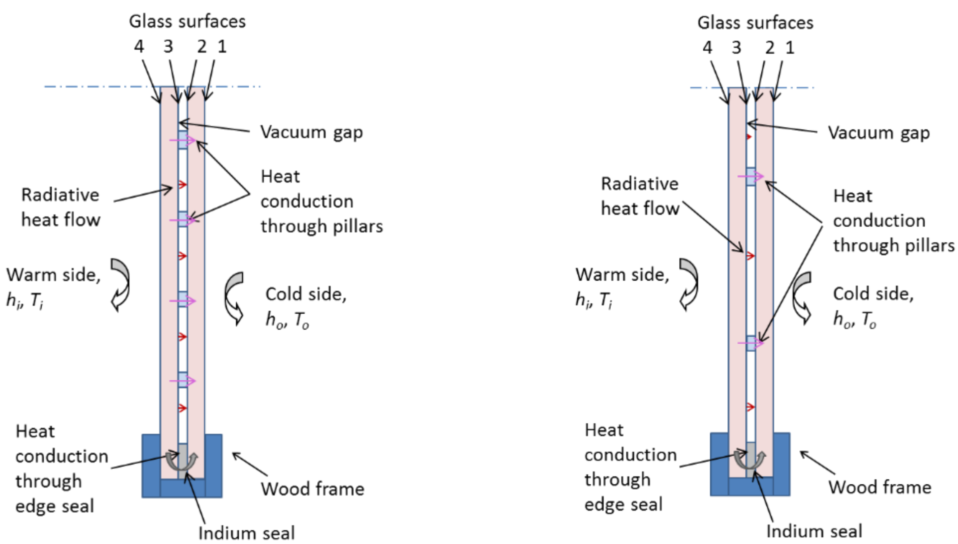


(2a) (2b)

**Fig. 2** Schematics (not to scale) of DEG with A-glass (1a) and T-glass (2b). The pillar separation in Fig. 2b is twice that in Fig. 2a.

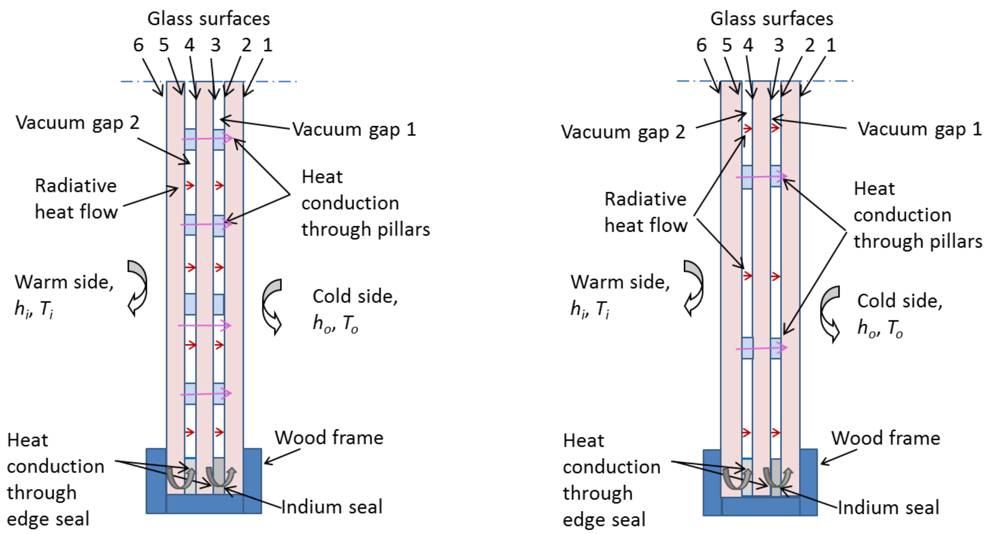


(3a) (3b)

**Fig. 3** Schematics (not to scale) of TEG with A-glass (3a) and T-glass (3b) glass. The pillar separation in Fig. 3b is twice that in Fig. 3a.

Analytical and finite element models of heat transfer through DEG and TEG have been experimentally validated (Collins and Simko, 1998; Fang et al., 2016). They are employed to analyze the heat transfer though the U-value of DEG and TEG and their comparison in this work.

## 2.2 Analytical model of DEG and TEG

Analytical models of DEG and TEG have been investigated by teams at Sydney (Collins and Simko, 1998) and at the Swiss Federal Laboratories (Manz et al., 2006), which were compared with numerical models developed by Sydney, Swiss and Ulster University teams independently (Fang et al., 2014). The simulation results by both analytic and finite volume models (FVM) were experimentally validated (Collins and Simko, 1998; Fang et al., 2014). The details of this work can be accessed in the literature. The analytical models clearly show that the larger the pillar separation, the lower the heat conduction contribution to the total heat transfer through the pillar arrays of DEG and TEG. This work modified these validated models to suit the specifications of DEG and TEG with a pillar separation twice that of conventional DEG and TEG with A-glass.

## 2.3 Finite volume model of DEG and TEG

The finite volume model was developed to simulate the thermal performance of DEG (Fang et al., 2014) and was further adapted to suit the structure of TEG (Fang et al., 2015). The sparse well structured system of equations of the FVM can be efficiently solved (Fang et al., 2014). This enables a large number of volumes to be employed to represent the DEG and TEG geometry and allow the direct representation of the small pillars. The DEG and TEG geometry and the small support pillars can then be represented by a large number of volumes. The equation bandwidth using the FVM method is smaller than that obtained for the FEM method and consequently requires fewer numeric operations and less CPU time to obtain a satisfactory solution. Only one quarter of the DEG and TEG was simulated to represent the whole glazing system under the ISO ambient conditions (ISO, 2017) since both DEG and TEG are symmetric. In the 3-D FVM, the support pillars were integrated and modelled into the complete system for ease of computation in the simulation. The cubical pillars were employed in the simulation to represent the cylindrical pillars in the practically fabricated DEG and TEG. The cubical and cylindrical pillars have the same areas of cross section, since both pillar shapes conduct similar amounts of heat under the same boundary conditions (ISO, 2017). The length of the square base of each cubical pillar is selected to be $\sqrt{\pi}a$, so as to keep the area of cross section of the cubical and cylindrical pillars the same, where $a$ is the radius of the equivalent cylindrical pillar. The mesh is optimized with a high density of nodes in and around each pillar to provide sufficient levels of accuracy to represent the heat transfer. In order to test the accuracy of simulations with specified mesh number, the thermal performance of a small central area (25 mm by 25 mm) with a single pillar in the centre was simulated using a mesh of 50×50×20 nodes for DEG and 50×50×30 for TEG. The mesh was denser in the area close to the pillar. The 20 and 30 nodes were distributed in a refined mesh through the glazing thickness of 8.2 mm for DEG and 12.4 mm for TEG. The thermal conductance of this simulated unit with a pillar in the centre was in good agreement with the analytic prediction with 1.5% and 1.8% variation for the DEG and TEG respectively, which are comparable to the results of Wilson et al (1998) and Manz et al., (2006). These levels of agreement indicate that the density of nodes is sufficient to simulate the realistic level of heat flow with high accuracy in DEG and TEG. The detailed description for the FVM model for DEG is presented in Fang et al., (2014).

With the 50×50 nodes distributed on the *y* and *z* directions on the glazing surface and with 20 nodes on the *x* direction, the thermal transmission at the centre-of-glazing for DEG with emittance of 0.03 was determined to be 0.36 $Wm^{-2}K^{-1}$ with a glass pane thickness of 6 mm. This is identical with the findings of Griffiths et al. (1998) thus this modelling approach is suitable to simulate a practical heat flow with high accuracy in TEG.

## 3. Simulated U-values of DEG and TEG with T-glass

The U-value of DEG and TEG (0.4 m by 0.4 m and 1 m by 1 m) with a 10 mm rebate depth in a solid wood frame were calculated under ISO standard winter boundary conditions (ISO, 2017) using a finite volume model. The evacuated glazing samples were assumed to have 6 mm wide metal edge seal and an array of support pillars with 0.4 mm diameter. The boundary conditions and parameters of DEG and TEG are listed in table 1.

**Table 1.** ISO (2017) winter boundary conditions used by the simulations of DEG and TEG.

| | Ambient temperature (°C) | Heat transfer coefficient ($Wm^{-2}K^{-1}$) |
|---|---|---|
| Warm side | 20 | 7.7 |
| Cold side | 0 | 25 |

The thermal conductivities of the metal edge seal, glass panes, stainless steel pillars and wood frame are 83.7 $Wm^{-1}K^{-1}$, 1 $Wm^{-1}K^{-1}$, 20.0 $Wm^{-1}K^{-}1$ and 0.14 $Wm^{-1}K^{-1}$, respectively.

### 3.1 The U-value of DEG with T-glass panes

Since the mechanical strength of T-glass is four to ten times stronger than A-glass, even if the pillar separation is significantly increased, the tensile stress on the external surface of glass panes above support pillars will not cause mechanical fracture within the service time of the evacuated glazing. Collins et al., (1999) reported that for 4 mm thick A-glass, the usual pillar space is between 20 to 25 mm and for 4mm T-glass, the pillar spacing can be increased to 54 mm. In this work, the pillar space of 50 mm is employed for both DEG and TEG with 4 mm thick T-glass panes. The 3-D isotherms on the warm and cold side glass panes of DEG with A-glass and T-glass panes coated with low-e coatings of 0.03 emissivity were calculated using the FVM and presented in Figs. 4 and 5.

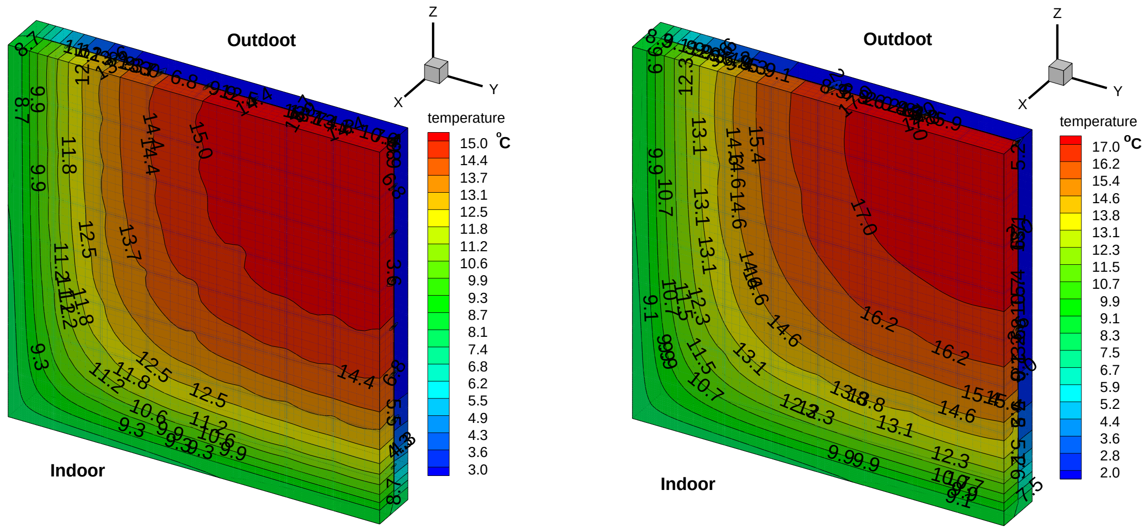


(4a) (4b)

**Fig. 4** 3-D isotherms of DEG with A-glass (4a) and T-glass (4b) with 0.03 emittance low-e coatings.

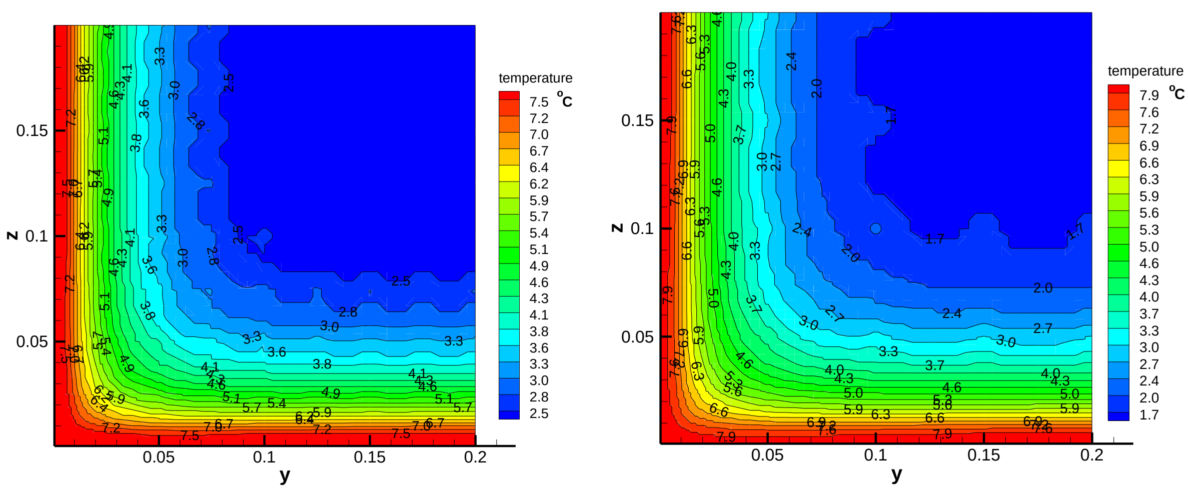


(5a) (5b)

**Fig. 5** Isotherms of the cold side glass panes of DEG with A-glass (5a) and T-glass (5b).

Figure 4(a) shows that the mean temperature at the centre-of-glazing area of DEG with A-glass is 15°C and Fig. 4(b) shows the temperature at the centre-of-glazing area of DEG with T-glass is 17°C which is clearly higher than that of the DEG with A-glass. Fig. 5(a) shows that the mean temperature at the centre-of-glazing region of the cold side surface of DEG with A-glass is 2.5°C and Fig. 5(b) shows that the mean temperature at the centre-of-glazing area of the cold side surface of the DEG with T-glass is 1.7 °C. Since the temperature of the warm side glass pane of the DEG with T-glass is higher than that of the DEG with A-glass and the temperature of the cold side glass pane of the DEG with T-glass is lower than that of the DEG with A-glass, DEG with T-glass provides enhanced insulation properties than DEG with A-glass panes.

In Figure 6, the dotted lines are the temperature lines on the cold and warm side glass surface right above one row of support pillars of the DEG with A-glass and the solid lines are the temperature lines on the cold and warm side glass surfaces right above one row of support pillars of the DEG with T-glass. The emittance of low-e coating on the A-glass and T-glass are 0.03.

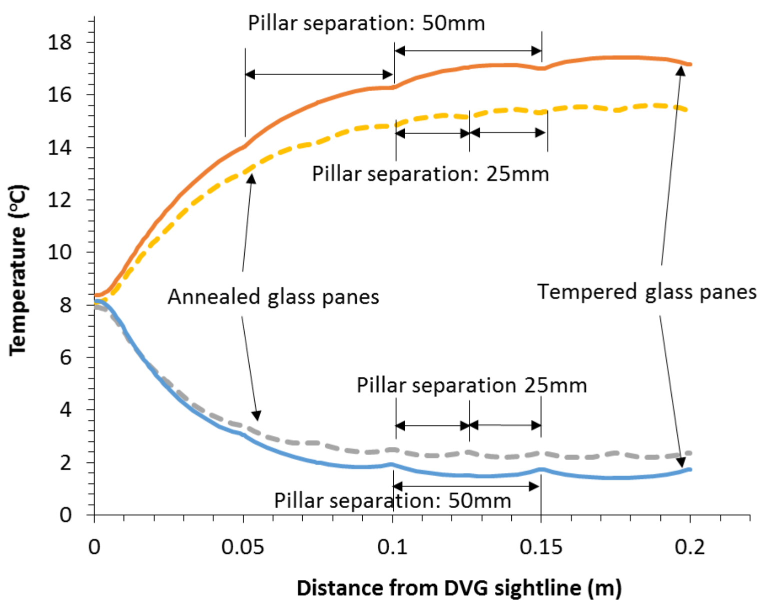


**Fig. 6** Comparison of temperature profiles of the 0.4 m by 0.4 m DEG with A-glass and T-glass coated with 0.03 emittance coatings.

Both dotted and solid temperature lines in Figure 6 are periodical. The variation period of the dotted lines is 25 mm and that of solid lines is 50 mm. These resulted from the heat conduction through the support pillars of DEG with 25 mm pillar spacing for DEG with A-glass and with 50 mm pillar spacing for the DEG with T-glass. The distance between the two solid lines at the cold and warm side glass panes is clearly larger than that of between the two dotted lines, which indicates the DEG with the T-glass (corresponding to solid lines) exhibits apparently higher thermal insulation than the DEG with A-glass (corresponding to dotted lines). The U-value of 0.4 m by 0.4 m and 1 m by 1 m DEG with A-glass and T-glass are calculated using FVM and presented in table 2. In table 2, U stands for U-value, the subscript

"T,c" stand for "centre-of-glazing area of T-glass pane", "A,c" stands for "centre-of-glazing area of A-glass panes", "T,t" stands for " total area of T-glass pane", "A,t" stands for "total glazing area of A-glass panes" and "Imp" represents "improvement".

**Table 2**. U-values of 0.4 m by 0.4 m ($A_1$) and 1 m by 1 m ($A_2$) DEG with T-glass and A-glass coated with 0.03 emittance low-e coatings.

| Glazing size | U centre-of-glazing (W $m^{-2}$ $K^{-1}$) | | Imp. (%) | U total glazing (W $m^{-2}$ $K^{-1}$) | | Imp. (%) |
|---|---|---|---|---|---|---|
| | $U_{T,c}$ | $U_{A,c}$ | | $U_{T,t}$ | $U_{A,t}$ | |
| $A_1$ | 0.30 | 0.57 | 47.4 | 0.53 | 0.73 | 27.4 |
| $A_2$ | 0.30 | 0.57 | 47.4 | 0.48 | 0.69 | 30.4 |

Table 2 shows that the improvement in the U-value at the centre-of-glazing area of both 0.4 m by 0.4 m and 1 m by 1 m DEG with T-glass compared to DEG with A-glass is 47.4% and the improvement in the U-value of total glazing area of 0.4 m by 0.4 m DEG due to the use of T-glass compared to DEG with A-glass is 27.4%. Due to the influence of heat conduction through the edge seal, the improvement (27.4%) in the U-value of total glazing is lower than that (47.4%) at the centre-of-glazing area, but it is still considerably good performance improvement. The improvements in the U-value of total glazing area of 1 m by 1 m DEG with T-glass compared to DEG with A-glass is 30.4%. Replacing A-glass with T-glass panes in 1 m by 1 m DEG achieves a larger improvement (30.4%) in the U-value of total glazing are compared to that (27.4%) of a smaller sized DEG.

### 3.2 The U-value of TEG with T-glass

The 3-D isotherms of TEG facing the warm and cold side for TEG made with A-glass and T-glass coated with low-e coatings of 0.03 emissivity were calculated and presented in Figures 7 and 8.

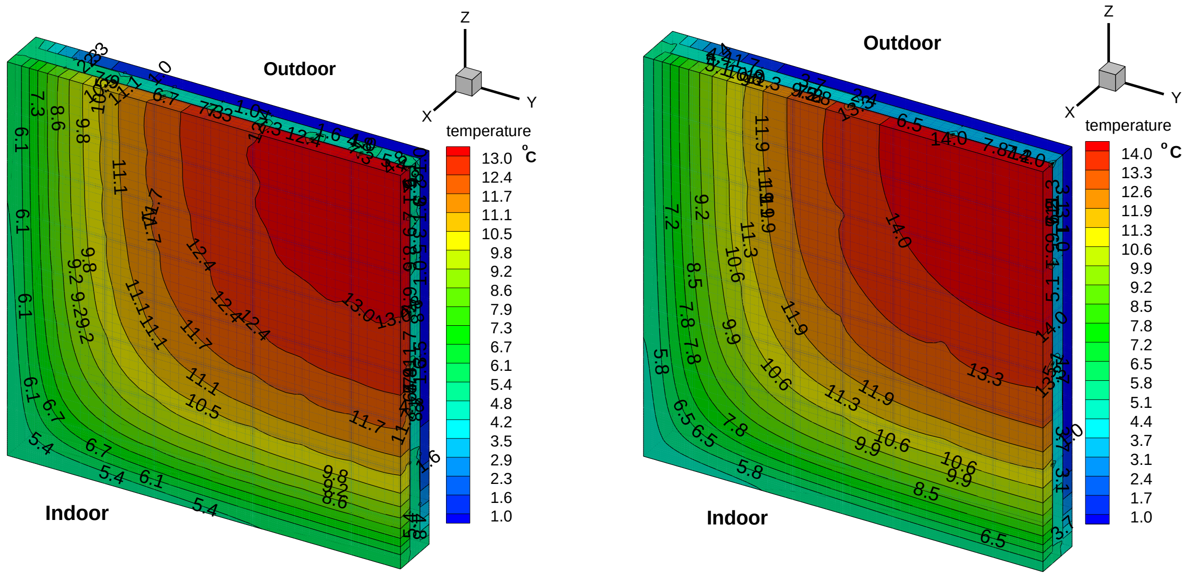


(7a) (7b)

**Fig. 7** 3-D Isotherms of TEG with A-glass (7a) and T-glass (7b).

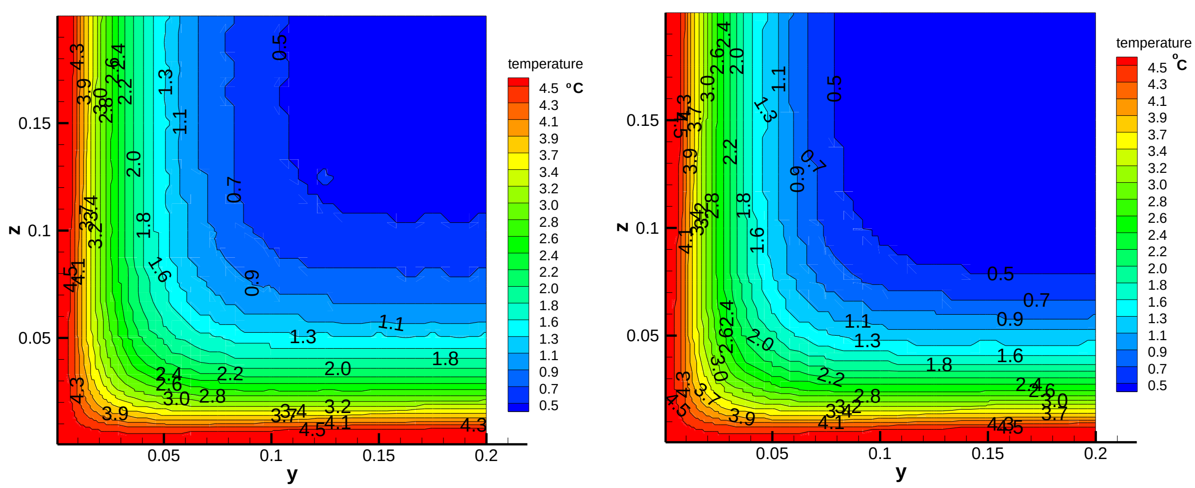


(8a) (8b)

**Fig. 8** Isotherms of the cold side glass panes of TEG with A-glass (8a) and T-glass (8b).

Figures 7(a) and 7(b) show that the mean temperature (14 ºC) at the centre-of-glazing region of the warm side pane of the TEG with T-glass shown in Fig. 7(b) is higher than that (13 ºC) of the TEG with A-glass shown in Fig. 7(a). Fig. 8 shows that the T-glass TEG has a larger area with a temperature less than 0.5ºC shown in Fig. 8(b) than TEG with annealed glass shown in Fig. 8(a). Consequently, the temperature difference between the warm and cold side glass of the T-glass TEG is significantly larger than that of the A-glass TEG, thus it provides enhanced thermal insulation compared to the A-glass TEG.

In Figure 9, the dotted lines are the temperature lines on the cold and warm side glass surface right above one row of support pillars of the TEG with A-glass panes, and the solid lines are the temperature lines on the cold and warm side glass surfaces right above one row of support pillars of the DEG with T-glass. Both T-glass and A-glass panes had low-e coatings of 0.03 emissivity.

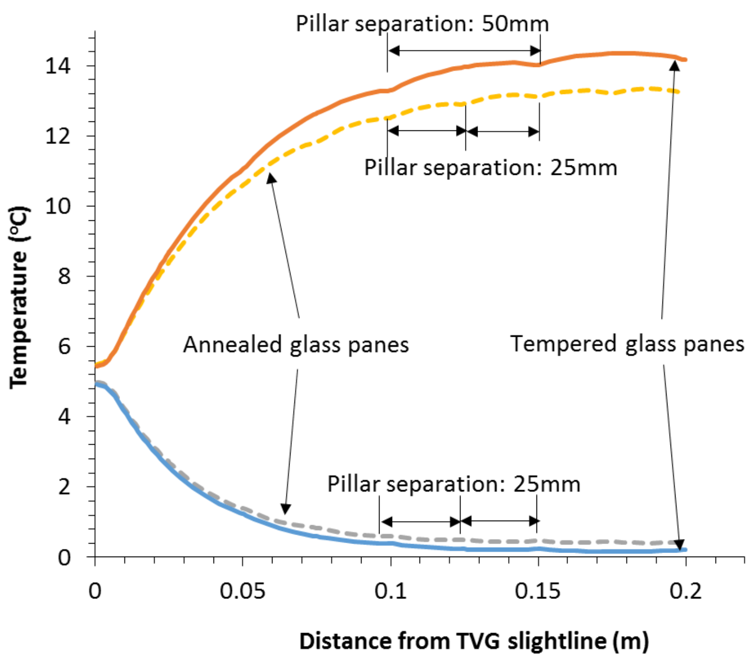


**Fig. 9** Comparison of the temperature profiles of 0.4 m by 0.4 m TEG with A-glass and T-glass.

In Figure 9 both dotted and solid temperature lines are periodically distributed. The variation period of the dotted lines is 25 mm and that of solid lines is 50 mm. These resulted from the heat conduction through the support pillars of TEG with 25 mm pillar spacing for TEG with A-glass and with 50 mm pillar spacing for the TEG with T-glass. The distance between the two solid lines at the cold and warm side glass panes is clearly larger than that of between the two dotted lines, which indicates the TEG with the T-glass (corresponding to solid lines) exhibits apparently higher thermal insulation than the TEG with A-glass (corresponding to dotted lines). The U-values of 0.4 m by 0.4 m and 1 m by 1 m TEG with A-glass and T-glass are calculated using FVM and presented in table 3.

**Table 3.** U-values of 0.4 m by 0.4 m ($A_1$) and 1 m by 1 m ($A_2$) TEG with T-glass and A-glass.

| Glazing size | U centre-of-glazing ($W\ m^{-2}\ K^{-1}$) | | Imp. (%) | U total glazing ($W\ m^{-2}\ K^{-1}$) | | Imp. (%) |
|---|---|---|---|---|---|---|
| | $U_{T,c}$ | $U_{A,c}$ | | $U_{T,t}$ | $U_{A,t}$ | |
| $A_1$ | 0.11 | 0.28 | 60.7 | 0.57 | 0.69 | 17.4 |
| $A_2$ | 0.11 | 0.28 | 60.7 | 0.40 | 0.52 | 23.1 |

Table 3 shows that the improvements in the U-value at the centre-of-glazing area of both 0.4 m by 0.4 m and 1 m by 1 m TEG with T-glass compared to TEG with A-glass is 60.7% and the improvements in the U-value of the total glazing of 0.4 m by 0.4 m TEG due to the use of T-glass compared to TEG with A-glass is 17.4%. The improvement (17.4%) in the U-value of total glazing is lower than that (60.7%) at the centre-of-glazing area, this is because the influence of heat flow through the edge seal is significant. The improvements in U-value of total glazing of 1 m by 1 m TEG with T-glass compared to TEG with A-glass is 23.1%. Replacing A-glass with T-glass panes in 1 m by 1 m TEG achieves a larger improvement (23.1%) in U-value of total glazing compared to that (17.4%) of a smaller sized TEG. This is because the influence of heat conduction through the edge on U-value of total glazing area of the 1 m by 1 m TEG is lower compared to that of the 0.4 m by 0.4 m TEG.

## 4. Further work on DEG with T-glass

Despite the fact that fabricated DEG with tempered glass panes coated with two low-e coatings with emissivity of 0.16 exhibited a U-value significantly lower than the best performing conventional double glazing (0.69 $W.m^{-2}.K^{-1}$ compared to 1.0 $W.m^{-2}.K^{-1}$), challenges during the fabrication process may prevent adoption of the fabrication methodology by industry for production lines. To predict the potential maximum bending of the glass panes between the support pillars, finite element software (ABAQUS) was used to simulate a vacuum glazing with the same specifications of the fabricated sample; (a pillar diameter of 0.4 mm, height of 0.15 mm, spacing of 50 mm, Young's Modulus of 70 GPa and Poisson's Ratio of: 0.22) the results of which are presented in Figure 10. Due to bending of the glass panes under atmospheric pressure, the glass panes would approach each other, however, a minimum separation of 0.05 mm would be maintained between the panes at a pillar spacing of 50 mm. Although this separation is acceptable, the distortion caused by roller wave could still result in contact points between the glass panes. Chemically toughened glass panes may help to solve this problem as the chemical toughening process does not affect the flatness of the glass panes (XINOLOGY, 2018).

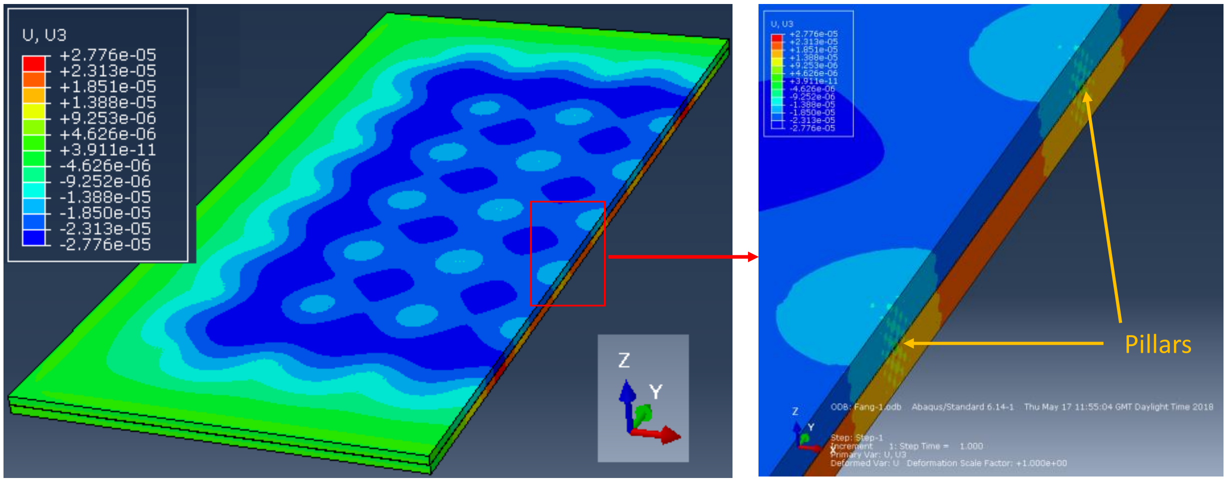


**Fig. 10** Bending profile for DEG with T-glass under atmospheric pressure.

## 5. Conclusions

Evacuated glazing is a thin glazing with high insulation characteristics suitable for application in energy efficient buildings and retrofitting to existing buildings, minimising heat lost or gain through windows. The fabrication of EG at low temperature allows the use of tempered glass in the fabrication of evacuated glazing without losing the mechanical properties of T-glass. The use of T-glass in evacuated glazing enables the increase of space between the support pillars without compromising the integrity of glazing. The increased pillar spacing reduces the number of pillars thereby reducesing the heat transfer across the glazing. Using annealed glass in vacuum glazing allows a pillar spacing of 25 mm (for a 0.4mm diameter pillar) without creating micro cracks in the glass at contact points, but research has shown that by using tempered glass in vacuum glazing it is possible to increase pillar spacing to over 50 mm.

In this work, the U-value of DEG and TEG was predicted for a glazing size of 0.4 m by 0.4 m and 1 m by 1 m. The simulated glazing used T-glass and A-glass separated by support pillar array spaced at 50 mm and 25 mm. The simulation showed that DEG made of A-glass with an emissivity of 0.03 had a thermal transmittance of 0.57 $W.m^{-2}.K^{-1}$ at the centre-of-glazing region while this reduced to 0.3 $W.m^{-2}.K^{-1}$ for DEG made of tempered glass (47.4% reduction). TEG using A-glass with an emissivity of 0.03 had a thermal transmittance of 0.28 $W.m^{-2}.K^{-1}$ at the centre-of-glazing region while this reduced to 0.11 $Wm^{-2}K^{-1}$ for TEG with T-glass (60.7% reduction).

It is apparent that using tempered glass in DEG and TEG can improve the thermal performance, however, the improvement for TEG was greater. Heat transfer by radiation in TEG is much lower than that in DEG therefore the heat conduction through the pillar array is more significant in TEG compared to DEG and as a result by reducing the number of the support pillars in TEG, the reduction in heat transfer across the total glazing would be larger.

The reduction in the thermal transmittance of larger sized DEG and TEG caused by the application of T-glass is greater than that of smaller sized glazing. The impact of heat transfer through the edge seal is larger in smaller sized DEG and TEG, thus the impact of the heat transfer through the support pillars on the overall thermal transmittance of 1 m by 1 m DEG and TEG is greater than that across the 0.4 m by 0.4 m DEG and TEG.

Since building regulations in many countries have required the use of T-glass for window and glazed façade of buildings, the detailed analysis for the thermal performance of DEG and TEG with T-glass under ISO winter conditions undertaken in this work will contribute to the development and application of evacuated glazing with T-glass.

## Nomenclature

| | |
|---|---|
| $T$ | Temperature (ºC) |
| $U$ | Thermal transmission ($W.m^{-2}.K^{-1}$) |

Subscripts

| | |
|---|---|
| *1 to 6* | Refer to surfaces of glass panes shown in Figs. 1 and 2 |
| *A,c* | Annealed glass and centre-of-glazing |
| *A,t* | Annealed glass and total glazing area |
| *i,o* | Refer to warm and cold side ambient |
| *T, c* | T-glass and centre-of-glazing |
| *T, t* | Tempered glass and total glazing area |

## ACKNOWLEDGEMENT

The support from Pump-Prime project from Coventry University is appreciated.

## References

Arya, Farid, 2014. Developing alternative sealing materials in fabrication of evacuated glazing at low temperature. Thesis (PhD). Ulster University. http://ethos.bl.uk/OrderDetails.do?uin=uk.bl.ethos.629079

Collins R.E., Asano O., Misonou M., Katoh H., Nagasaka S., 1999. Vacuum glazing: design option and performance capability. Proceeding of Glass in Buildings Conference Bath U.K. pp221-226.

Collins RE, Simko TM., 1998. Current status of the science and technology of vacuum glazing. Solar Energy 62 189-213. doi:10.1016/S0038-092X(98)00007-3

Collins R.E., Robinson S.J., 1991. Evacuated glazing. Solar Energy 47 27-38. doi:10.1016/0038-092X(91)90060-A.

Collins, R.E., Fischer-Cripps, A.C. And Tang, J.Z., 1992. Transparent evacuated insulation. Solar Energy, 49(5), pp. 333-350.

Cuce E., Cuce P.M., Young C.H., 2016. Energy saving potential of heat insulation solar glass: Key results from laboratory and in-situ testing. Energy 97 369-380. http://dx.doi.org/10.1016/j.energy.2015.12.134

Cuce E., Cuce P.M., 2016. Vacuum glazing for highly insulating windows: Recent developments and future prospects. Renewable and Sustainable Energy Reviews 54 1345-1357. doi: 10.1016/j.rser.2015.10.134

Fang Y., Hyde T.J., Arya F., Hewitt N., 2013. A novel building component hybrid vacuum glazing-a modeling and experimental validation. ASHRAE, Volume 119, Part 2.

Fang Y., Hyde T.J., Arya F., Hewitt N., Eames P. C., Norton B., Miller S., 2014. Indium alloy-sealed vacuum glazing development and context. Renewable and Sustainable Energy Review 37 480-501. http://dx.doi.org/10.1016/j.rser.2014.05.029

Fang Y., Hyde T.J., Arya F., Hewitt N., Wang R., Dai Y., 2015. Enhancing the thermal performance of triple vacuum glazing with low emittance coatings. Energy and Buildings 97 186–195 doi:10.1016/j.enbuild.2015.04.006

Frost K., Eto J., Arasteh D., Yazdanian M., 1996. The national energy requirements of residential windows in the US: today and tomorrow. In: ACEE Proceedings on energy efficiency in buildings; August 1996, Pacific Grove, Canada.

Fung T.Y.Y., Yang H., 2008. Study on thermal performance of semi-transparent building-integrated photovoltaic glazings. Energy and Buildings 40 341-350. doi:10.1016/j.enbuild.2007.03.002

Ghosh A., Norton B., Duffy A. 2016. Measured thermal performance of a combined suspended particle switchable device evacuated glazing. Applied Energy 169 469–480. http://dx.doi.org/10.1016/j.apenergy.2016.02.031

Griffiths PW, Leo M di, Gartwright, Eames P.C., Yianoulis P., Leftheriotis G., Norton B., 1998. Fabrication of evacuated glazing at low temperature. Solar Energy 63 243-9. doi:10.1016/S0038-092X(98)00019-X

Hyde T.J., Griffiths P.W., Eames P.C., Norton B., 2000. Development of a novel low temperature edge seal for evacuated glazing. Pro. World Renewable Energy Congress VI, Brighton, U.K. pp271-274.

ISO 10077-1, 2017. Thermal performance of windows, door, and shutters – calculation of thermal transmittance – part 1: simplified method. Brussels.

LandVac Website accessed on 16 Feb 2019 through: https://www.landvac.net/product.php

Peng J., Curcija D.C., Lu L., Selkowitz S.E., Yang H., Zhang W., 2016. Numerical investigation of the energy saving potential of a semi-transparent photovoltaic double-skin facade in a cool-summer Mediterranean climate. Applied Energy, 165, 345-356. doi.org/10.1016/j.apenergy.2015.12.074.

Pilkington, 2019. Website accessed on 16 Feb 2019 through: https://www.pilkington.com/en-gb/uk/products/product-categories/thermal-insulation/pilkington-spacia#brochures

Jelle B.P., Hynd A., Gustavsen A., Arasteh D., Goudey H, Hart R., 2012. Fenestration of today and tomorrow: A state-of-the-art review and future research opportunities. Solar Energy Materials and Solar Celles 96 1-28. doi:10.1016/j.solmat.2011.08.010

Manz H., Menti U., 2012. Energy performance of glazing in European climates. Renewable Energy 37 226–232. doi:10.1016/j.renene.2011.06.016

Manz H., 2008. On minimizing heat transfer in architectural glazing. Renewable Energy 33 119-128. doi:10.1016/j.renene.2007.01.007

Manz H., Brunner S., Wullschleger L., 2006. Triple vacuum glazing: Heat transfer and basic mechanical design constrains. Solar Energy 80 1632-42. doi:10.1016/j.solener.2005.11.003

Shen C, Li X., 2016. Solar heat gain reduction of double glazing window with cooling pipes embedded in venetian blinds by utilizing natural cooling. Energy and Buildings 112 173-183. doi:10.1016/j.enbuild.2015.11.073

Schultz J.M., Jensen K.I., Kristiansen F.H., 2005. Super insulation aerogel glazing. Solar Energy Materials and Solar Cells 89 275-285. doi:10.1016/j.solmat.2005.01.016

Wang M., Peng J., Li N., Yang H., Wang C., Li X., Lu T., 2017. Comparison of energy performance between PV double skin facades and PV insulating glass units. Applied Energy. 194, 148-160. doi.org/10.1016/j.apenergy.2017.03.019

Wang T.P., Wang L.B., 2016. The effects of transparent long-wave radiation through glass on time lag and decrement factor of hollow double glazing. Energy and Buildings 117 33-43. http://dx.doi.org/10.1016/j.enbuild.2016.02.009

Wilson CF, Simko TM, Collins RE. Heat condiction through the support pillars in vacuum glazing, 1998. Solar Energy. 63, 393-406. doi:10.1016/S0038-092X(98)00079-6.

Xinology 2018 Accessed on 5th December 2018 at: http://www.xinology.com/Glass-Mirrors-Products/chemical-strengthen/overview/vs-thermal-temper-glass.html.

Zhao, J., Eames, P.C., Hyde T., Fang Y., Wang J., 2007. A modified pump-out technique used for fabrication of low temperature metal sealed vacuum glazing. Solar Energy, 81, 1072-1077. doi:10.1016/j.solener.2007.03.006.